Published online 18 March 2010 *Nucleic Acids Research, 2010, Vol. 38, No. 13* ***4263–4273***
doi:10.1093/nar/gkq171

Identification and characterization of the two isoforms of the vertebrate H2A.Z histone variant

Ryo Matsuda[1], Tetsuya Hori[2], Hiroshi Kitamura[1], Kozo Takeuchi[2], Tatsuo Fukagawa[2] and Masahiko Harata[1,*]

[1]Laboratory of Molecular Biology, Graduate School of Agricultural Science, Tohoku University, Tsutsumidori-Amamiyamachi 1-1, Aoba-ku, Sendai 981-8555 and [2]Department of Molecular Genetics, National Institute of Genetics and The Graduate University for Advanced Studies, Mishima 411-8540, Japan

Received November 5, 2009; Revised February 25, 2010; Accepted March 3, 2010

ABSTRACT

Histone variants play important roles in the epigenetic regulation of genome function. The histone variant H2A.Z is evolutionarily conserved from yeast to vertebrates, and it has been reported to have multiple effects upon gene expression and insulation, and chromosome segregation. Recently two genes encoding H2A.Z were identified in the vertebrate genome. However, it is not yet clear whether the proteins transcribed from these genes are functionally distinct. To address this issue, we knocked out each gene individually in chicken DT40 cells. We found that two distinct proteins, H2A.Z-1 and H2A.Z-2, were produced from these genes, and that these proteins could be separated on a long SDS–PAGE gel. The two isoforms were deposited to a similar extent by the SRCAP chromatin-remodeling complex, suggesting redundancy to their function. However, cells lacking either one of the two isoforms exhibited distinct alterations in cell growth and gene expression, suggesting that the two isoforms have differential effects upon nucleosome stability and chromatin structure. These findings provide insight into the molecular basis of the multiple functions of the H2A.Z gene products.

INTRODUCTION

The genomes of eukaryotic organisms are packaged into chromatin. Chromatin is composed of nucleosomes, in which DNA is wrapped around a histone octamer containing two copies of each of the H2A, H2B, H3 and H4 histones (1,2). The modification of chromatin structure contributes to the regulation of DNA transcription, replication and repair, as well as the process of chromosomal segregation. ATP-dependent chromatin remodeling complexes and post-translational modification of core histones by modification complexes have been intensively investigated with the aim of gaining a better understanding of the molecular mechanisms underlying this regulation. The replacement of canonical histones within the chromatin by structurally similar histone variants via intrinsic chromatin-remodeling complexes has recently been shown to affect genome function (3,4).

H2A.Z is one of the more highly conserved histone variants in eukaryotes. While H2A.Z is not essential for the growth of yeast, it is essential for the survival of *Tetrahymena* (5) and early development in *Drosophila* and the mouse (6,7). The SWR1 chromatin-remodeling complex is responsible for the deposition of H2A.Z into chromatin in yeast (8). The SRCAP chromatin-remodeling complex, which is the vertebrate counterpart of the yeast SWR1 complex, is also capable of H2A.Z deposition. However, in contrast to the situation in yeast, the p400 protein complex is also able to deposit H2A.Z into vertebrate chromatin. It is not clear whether differences exist between the mechanisms of H2A.Z deposition by the SRCAP and p400 complexes (8–10).

H2A.Z has multiple functions in both yeast and vertebrates. The localization of H2A.Z within gene promoters and insulator regions has been reported (11–16). H2A.Z regulates gene expression when localized to promoter regions. Recently, it has also been shown that H2A.Z plays important roles in regulating epigenetic memory (17) and in suppressing read-through antisense transcription (18). H2A.Z localized within insulator regions antagonizes the spread of heterochromatin (14). In higher eukaryotes, H2A.Z co-localizes with the heterochromatin protein HP1α (19,20), suggesting roles in the organization of heterochromatin. In addition, inhibition of the expression of H2A.Z by using RNAi affects both genome stability and chromosome segregation (20).

Analysis of chromatin proteins from yeasts to vertebrates reveals the evolution of isoforms in vertebrates that contribute to biological processes such as

*To whom correspondence should be addressed. Tel: +81 22 717 8771; Fax: +81 22 717 8883; Email: mharata@biochem.tohoku.ac.jp

development and differentiation. For example, the actin-related protein, Arp4, which is a common component of the SRCAP and p400 complexes, exists as two isoforms (ArpNα/BAF53b and ArpNβ/BAF53a) only in vertebrates, with the latter specific to the brain. Mammalian cells contain three isoforms of histone H3 (H3.1, H3.2 and H3.3), whereas yeast contains only one. In mammals, H3.1 and H3.3 differ by a mere five and four residues, respectively. H3.1 and H3.2 are associated with silent genes, whereas H3.3 is associated with actively transcribed genes (21). Interestingly, recent genome-wide analyses of histone variants in higher eukaryotes have revealed that H3.3 co-localizes with H2A.Z in nucleosomes within transcriptional regulatory elements (16,22). It has been suggested that H3.3/H2A.Z-containing nucleosomes are more labile and more easily displaced by transcription factors (16,22,23).

Whereas a single gene (*HTZ1*) encodes H2A.Z in budding yeast, two genes have been identified in vertebrates. These were named *H2A.Z-1* (previously *H2A.Z*) and *H2A.Z-2* (previously *H2A.F/Z* or *H2A.V*) (24,25). Although most studies to date have evaluated the product of the *H2A.Z-1* gene, two distinct H2A.Z isoforms corresponding to *H2A.Z-1* and *H2A.Z-2* have been identified by mass spectrometry (25,26). Interestingly, the N-terminal tails of H2A.Z-1 and H2A.Z-2 are similarly acetylated and ectopically expressed H2A.Z-2 preferentially associates with H3 that is trimethylated at lysine 4 (26,27). However, it is not clear whether the two isoforms have redundant and/or different properties and functions.

In this report, we describe the establishment of DT40 cells in which either the *H2A.Z-1* or *H2A.Z-2* gene has been knocked out, enabling us to identify gene products corresponding to the two distinct H2A.Z isoforms. We show that the two H2A.Z isoforms are deposited into chromatin by a similar mechanism, indicating a redundancy to their processing. However, the two knockout lines exhibit different phenotypes with regard to cell growth and gene expression. These two knockout lines should prove useful to investigate the redundant and differential functions of the H2A.Z isoforms.

MATERIALS AND METHODS

Analyses of amino acid and nucleotide sequences

The amino acid and nucleotide sequences of histones and H2A.Z isoforms were analyzed using various bioinformatics tools, including similarity search BLAST (http://www.ncbi.nlm.nih.gov/blast) and phylogenetic prediction by ClustalW (http://www.ebi.ac.uk/clustalw) for each query DNA sequence.

Cell culture

DT40 and CEF cells were cultured at 38°C in Dulbecco's modified medium supplemented with 10% fetal calf serum, 1% chicken serum, 2-mercaptoethanol, penicillin and streptomycin. HeLa and MEF cells were cultured at 37°C in Dulbecco's modified medium supplemented with 10% fetal calf serum, penicillin and streptomycin. Nalm6 cells were cultured at 37°C in Roswell Park Memorial Institute medium containing GlutaMAX™-I (Invitrogen) supplemented with 10% fetal calf serum, penicillin and streptomycin. To suppress expression of the tetracycline (tet)-responsive H2A.Z-1 transgene, tetracycline (Sigma) was added to the culture medium to a final concentration of 2 μg/ml.

Construction of plasmids

The chicken cDNAs for H2A.Z-1 and H2A.Z-2 were cloned by screening a chicken testis cDNA library (Stratagene) with reverse transcriptase (RT)-PCR products as probes. The cDNAs for H2A.Z-1 and H2A.Z-2 were used as probes to isolate genomic clones for *H2A.Z-1* and *H2A.Z-2* genes from a DT40 genomic library. The left (4.0 kb) and right (4.1 kb) arms of the disruption construct for the first *H2A.Z-1* allele and also the left (5.0 kb) and right (1.0 kb) arms for the second *H2A.Z-1* allele were cloned in a similar fashion into pBluescript (KS+). For the disruption constructs, the mycophenol (EcoGpt) and blasticidin (bsr) resistance cassettes under control of the β-actin promoter were inserted between the two arms of these constructs, respectively. The full-length cDNA for H2A.Z-1 was cloned into the *Bam*HI site of pUHD10-3 (28) to yield a tetracycline-responsive expression plasmid, pUHD-H2A.Z-1. The left (3.0 kb) and right (3.7 kb) arms of the *H2A.Z-2* disruption constructs were cloned sequentially into pBluescript (KS+). For the disruption constructs, the histidinol (hisD) or puromycin (puro) resistance cassette under control of the β-actin promoter was inserted between the two arms.

Production of H2A.Z-1- and H2A.Z-2-deficient cells

Targeted disruption constructs for allelic *H2A.Z-1* genes were generated so that 1.3 kb genetic fragments encoding amino acids 2–128 (exons 2–5) and 0.4 kb genetic fragments encoding amino acids 6–28 (exons 2 and 3) were replaced with a mycophenol- (EcoGpt) resistance cassette and a blasticidin- (bsr) resistance gene under the control of the β-actin promoter, respectively. *H2A.Z-1* genes was sustained by expression of integrated *H2A.Z-1* genes under control of a tet-repressible promoter. The genotype of the resulting $H2A.Z\text{-}1^{-/-/H2A.Z\text{-}1\ transgene}$ cell line (*H2A.Z-1*-KO) was confirmed by PCR analysis. Targeted disruption constructs for the allelic *H2A.Z-2* gene were generated such that 0.4-kb genetic fragments encoding amino acids 2–64 (exons 2 and 3) were replaced with a histidinol- (hisD) or puromycin- (puro) resistance cassette under the control of the β-actin promoter. The genotype of the resulting $H2A.Z\text{-}2^{-/-}$ cell line (*H2A.Z-1*-KO) was confirmed by Southern blot analysis. The target constructs were transfected with the Gene Pulser II electroporator (Bio-Rad, Tokyo, Japan). Mycophenol (Invitrogen) at a final concentration of 2.5 μg/ml, xanthin at a final concentration of 0.5 mg/ml, blasticidin (Invitrogen) at a final concentration of 25 μg/ml, histidinol (Sigma) at a final concentration of 1 mg/ml and puromycin (Clontech) at a final concentration of 0.5 μg/ml were used to select stable transfectants.

Real-time PCR and quantitative PCR

Total RNA from HeLa, mouse embryonic fibroblast (MEF), and chicken DT40 cells was extracted with the RNeasy Mini kit (QIAGEN) according to the manufacturer's protocol. One microgram of the extracted RNA was incubated with 0.15 μg random primer in 20 μl deionized water for 5 min at 65°C and then chilled on ice. Then, 200 U superscript III reverse transcriptase (Life Technologies) and 28 U RNase inhibitor in 20 μl of 2× first strand buffer (Life Technologies) containing 20 mM DTT and 1 mM dNTPs were added, and first strand cDNA was synthesized by incubating the mixture for 50 min at 50°C. RT-PCR was carried out using gene specific primers for human *H2A.Z-1* (5′-TCCAGTGTTG GTGATTCCAG-3′ and 5′-GCAGAAATTTGGTTGGT TGG-3′), mouse (5′-CCAACCAACCAAATTTCTGC-3′ and 5′-CCACCAGAGTGGAAACAATG-3′) and chicken (5′-TATCTCAGGACTCTAAGTAC-3′ and 5′-C GGTTAAGACTTCAATGCAG-3′), and also primers for *H2A.Z-2* in human (5′-TCCCTCACATCCACAAAT CTC-3′ and 5′-AGTACAATGACGGGGAGGAA-3′), mouse (5′-GGTCTGTAACAGGGCAGAGG-3′ and 5′-CTGGCCAATCAACACATGAC-3′), and chicken (5′-AGGGAGGAAACGTTTCTATG-3′ and 5′-GGGA GAAACCTCAGCCAATC-3′). β-actin mRNA was also used as an internal control. For an accurate quantification of *H2A.Z-1* and *H2A.Z-2* mRNA, real-time RT–PCR was carried out by using the comparative CT method, according to the manufacture's instructions for the ABI prism 7000 sequence detection system.

Northern blot analysis

Total RNA was extracted from DT40 cells using TRIzol (Invitrogen) reagent according to the manufacturer's protocol. RNA (10 μg) was electrophoresed through a 1% agarose gel and transferred to a Hybond N+ membrane (Amersham Pharmacia Biotech). The blot was prehybridized in phosphate–SDS buffer (7% SDS, 1% bovine serum albumin, 1 mM EDTA, 0.5 M sodium phosphate), and then hybridized to ^{32}P-labeled antisense oligonucleotides corresponding to the H2A.Z-1 or H2A.Z-2 coding regions at 63°C overnight. The membrane was washed in wash buffer-1 (2× SSC, 0.5% SDS) and wash buffer-2 (0.5× SSC, 0.5% SDS) at 63°C for 30 min.

Preparation of histones and chromatin fraction

DT40 cells were washed in PBS, and cytoplasmic proteins and soluble nuclear proteins were extracted with lysis buffer (25 mM Hepes, 0.3 M NaCl, 0.2 mM EDTA, 2 mM $CaCl_2$, 0.5 mM DTT, 0.5% Triton) on ice for 3 min. Chicken embryos were homogenized with a Dounce homogenizer in RSB buffer (10 mM Tris–HCl, 10 mM NaCl, 3 mM $MgCl_2$). The remaining nuclei were recovered by centrifugation at 14 000 rpm for 10 min at 4°C. Histone proteins were extracted with acid extraction buffer (0.22 N H_2SO_4, 20% glycerol, 0.5 mM DTT), and the supernatant was added to 100% (w/v) trichloroacetic acid, and the pellets were recovered by centrifugation at 14 000 for 30 min at 4°C. The pellets were washed in acetone and then centrifuged. Histones were recovered as the remaining pellet. For the preparation of MNase-treated soluble chromatin, the nuclear pellet was suspended in lysis buffer, and chromatin was solubilized by DNA digestion with 0.5 U micrococcal nuclease (MNase, TaKaRa) for 40 min at 37°C.

Expression and purification of recombinant chicken H2A.Z proteins

Chicken *H2A.Z-1* and *H2A.Z-2* genes were cloned into the pET15b vector (Novagen). Recombinant proteins fused to the 6xHis-tag were expressed in *Escherichia coli* JM109(DE3) cells and were purified with a HisTrap FF column (GE Healthcare Biosciences) under denaturing conditions. The 6xHis-tag was removed from the purified proteins by digestion with thrombin protease. The H2A.Z protein isoforms were further purified using a MonoS column (GE Healthcare Biosciences). Purified H2A.Z-1 and H2A.Z-2 were dialyzed against H_2O and then lyophilized using a Speed-Vac concentrator (Tomy, Tokyo).

Western blot analysis

The protein samples were electrophoresed through a 28.5 cm long, 15% polyacrylamide gel (Nippon Eido) for 30 min at 11 mA and then 5 h at 25 mA, and the separated proteins were transferred to a PVDF membrane (Millipore). Western blot analysis was performed with an anti-H2A.Z antibody (Abcam ab4174) or an anti-H3 antibody (Abcam ab1791). An anti-IgG conjugated to horseradish peroxidase (Promega) was used as the secondary antibody, and ECL western blotting detection reagents (GE Healthcare) were used for the detection of bound antibodies.

RESULTS

Both H2A.Z-1 and H2A.Z-2 gene products are expressed in vertebrate cells

H2A.Z has been shown to play multiple roles in the epigenetic regulation of chromatin function. We have previously identified two genes encoding H2A.Z in mammals and chicken, which have recently been named *H2A.Z-1* and *H2A.Z-2* (24,26). Comparison of the deduced amino acid sequences of the gene products of H2A.Z-1 and H2A.Z-2 revealed that they differ by three and four residues in mammals and chicken, respectively (Supplementary Figure S1). The deduced amino-acid sequence of H2A.Z-2 is identical in all vertebrates analyzed, whereas that of H2A.Z-1 diverges slightly [(24) and Supplementary Figure S1]. Although most studies to date have evaluated the H2A.Z-1 isoform, the high degree of conservation of amino acid sequence of H2A.Z-2 implies that both isoforms play important roles in vertebrates.

To test whether both *H2A.Z-1* and *H2A.Z-2* gene products are expressed in vertebrate cells, we performed RT-PCR using primer sets that were specifically targeted

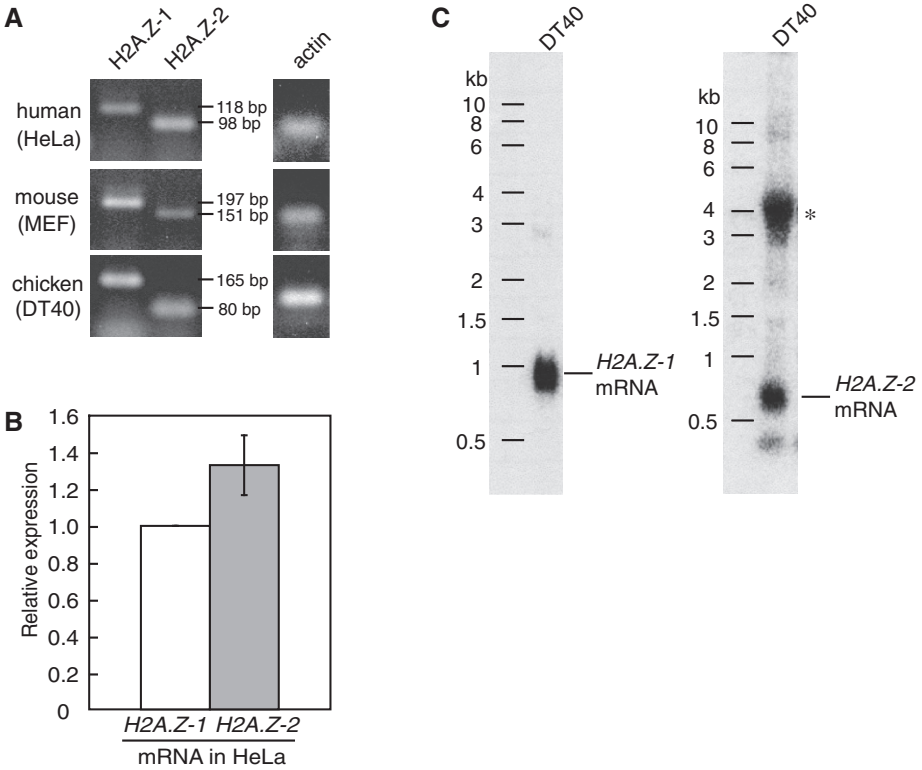

Figure 1. Expression of both of *H2A.Z-1* and *H2A.Z-2* genes in vertebrate cells. (**A**) Expression of *H2A.Z-1* and *H2A.Z-2* in HeLa, mouse embryonic fibroblast (MEF), and chicken DT40 cells was evaluated by RT-PCR using primer sets specific for the cDNAs of H2A.Z-1 and H2A.Z-2, respectively. The transcript encoding β-actin was monitored as a control. (**B**) Expression of *H2A.Z-1* and *H2A.Z-2* in HeLa cells was compared by real-time quantitative RT-PCR analysis. The relative levels of the amplified fragments corresponding to the transcripts encoding the H2A.Z isoforms were estimated by comparison to those derived from cloned cDNA fragments corresponding to each isoform. The relative expression of H2A.Z-2 to H2A.Z-1 was plotted. The error bars represent the mean ± standard deviation from three experiments. (**C**) Northern blot analysis of mRNAs encoding H2A.Z-1 and H2A.Z-2 from DT40 cells. Total RNA was electrophoresed through a formaldehyde gel and hybridized to a fragment corresponding to the coding region of H2A.Z-1 cDNA (left) or H2A.Z-2 cDNA (right). Fragments corresponding to mRNAs encoding H2A.Z-1 and H2A.Z-2 are indicated on the right. An asterisk indicates a nonspecific band, which was confirmed by using H2A.Z-2 knockout cells.

to the H2A.Z-1 or H2A.Z-2 cDNAs. We found that both genes are expressed in human, mouse and chicken cells (Figure 1A). The expression of the genes encoding the H2A.Z isoforms in HeLa cells was confirmed by quantitative RT-PCR (Figure 1B). In this analysis, the level of the real-time PCR products corresponding to mRNAs encoding H2A.Z-1 and H2A.Z-2 in HeLa cells was compared to that observed for cloned and quantified cDNAs in order to estimate the relative expression of the two endogenous genes. This analysis revealed that *H2A.Z-1* and *H2A.Z-2* genes were expressed at a similar level in HeLa cells (Figure 1B). Transcripts corresponding to the two H2A.Z gene isoforms were detected by northern blot analysis of RNA prepared from chicken DT40 cells (Figure 1C). Signals corresponding to the *H2A.Z-1* and *H2A.Z-2* transcripts were detected at positions corresponding to 1.0 and 0.7 kb, respectively. The apparent lengths of these RNAs are consistent with those of the predicted mature, full-length mRNAs. These observations suggest that both the H2A.Z-1 and H2A.Z-2 genes are expressed and appropriately processed in these vertebrates.

Electrophoretic separation and identification of H2A.Z-1 and H2A.Z-2 proteins

Analysis of the two H2A.Z protein isoforms requires a means to detect each molecule individually. Since the epitopes recognized by the available H2A.Z antibodies cannot distinguish between the H2A.Z isoforms, we tried to separate the H2A.Z-1 and H2A.Z-2 protein isoforms by electrophoresis. When the nuclear histone fraction isolated from various vertebrate cells was separated by electrophoresis through an acid–urea–Triton acrylamide (AUT) gel, a single band was identified following western blot analysis using an anti-H2A.Z antibody (Supplementary Figure S2). Electrophoresis through a conventional short SDS–PAGE gel also gave a single band (data not shown). However, separation of the protein samples on a long SDS–PAGE gel (28.5-cm long) allowed us to identify two distinct polypeptides in chicken cells (Figure 2A). This finding suggests that chicken H2A.Z-1 and H2A.Z-2 can be distinguished from one another due to a slight difference in mobility during prolonged analysis by SDS–PAGE. In contrast, it was not possible to identify two distinct human or mouse

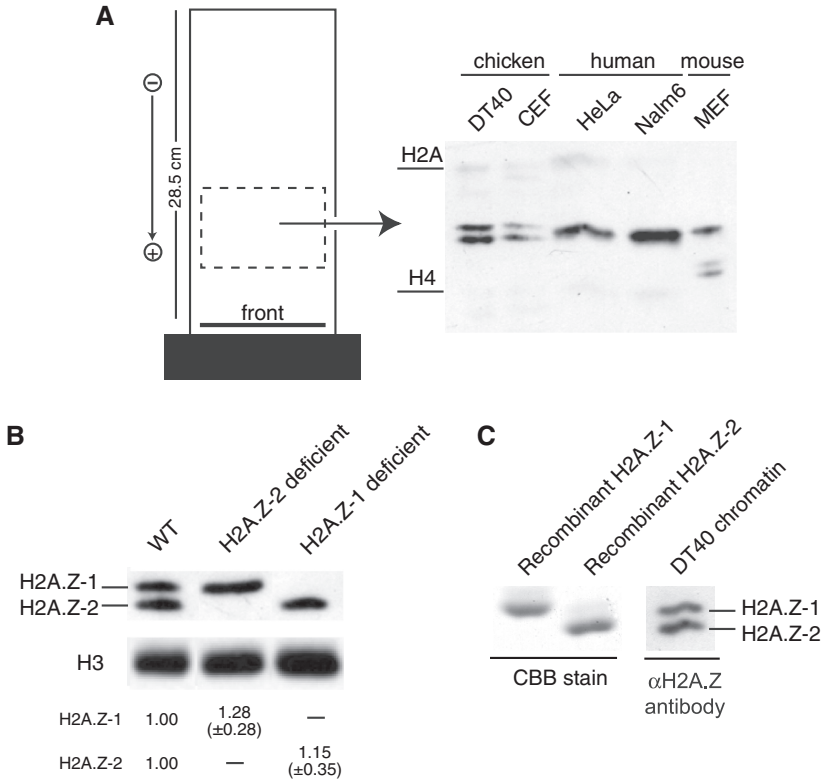

Figure 2. Electrophoretic separation and identification of chicken H2A.Z-1 and H2A.Z-2 proteins. (**A**) The nuclear histone fractions from chicken (DT40 and embryonic fibroblast; CEF), human (HeLa and Nalm6), and mouse (MEF) cells were prepared by acid extraction. Histones were electrophoresed through a 28.5 cm 15% acrylamide gel for 5 h at 25 mA. A gel piece containing the histones was subjected to western blot analysis and H2A.Z isoforms were detected using an anti-H2A.Z antibody. The positions of the H2A and H4 histones are indicated at the left. (**B**) Histones from WT, H2A.Z-1 deficient and H2A.Z-2 deficient cells were prepared, and H2A.Z-1, H2A.Z-2 and H3 histones were detected as in (A). The relative intensities of the signals corresponding to H2A.Z-1 or H2A.Z-2 to that of the H3 histone are shown with the relative signal in WT cells defined as 1.0. The mean ± standard deviation from at least three independent experiments is shown. (**C**) Bacterially expressed and purified H2A.Z isoforms (recombinant H2A.Z-1 and H2A.Z-2) were electrophoresed as in (A) and detected by Coomassie staining (left panel). Western blot analysis was used to compare the mobility of the recombinant H2A.Z isoforms to that of the endogenous proteins in the chromatin fraction prepared from DT40 cells (right panel).

H2A.Z polypeptides based on differential mobility during prolonged analysis by SDS–PAGE.

With the aim of identifying individually each chicken H2A.Z isoform by western blot analysis, we first generated individual gene knockouts of each isoform in chicken DT40 cells (Supplementary Figure S3). The *H2A.Z-1* alleles were disrupted using an *H2A.Z-1* transgene whose expression was under the control of a tetracycline (tet)-repressible promoter. We confirmed the genotype of the resulting $H2A.Z\text{-}1^{-/-/H2A.Z\text{-}1\ transgene}$ cells, including the disappearance of the mRNA corresponding to the H2A.Z-1 isoform in the presence of tet (Supplementary Figures S4 and S5). The cells were maintained in the presence of tet and were analyzed as H2A.Z-1-deficient cells. Similarly, we also confirmed the genotype of the H2A.Z-2-deficient cells ($H2A.Z\text{-}2^{-/-}$) and the disappearance of the mRNA corresponding to the H2A.Z-2 isoform in these cells (Supplementary Figures S4 and S5).

Histones prepared from these H2A.Z-deficient cells were subjected to western blot analysis following separation by long-gel SDS–PAGE (Figure 2B). While two distinct polypeptides were detected in wild-type (WT) cells, the higher-mobility (lower) polypeptide was absent from histones prepared from H2A.Z-2-deficient cells, and the lower-mobility (upper) polypeptide was absent from histones prepared from H2A.Z-1-deficient cells (Figure 2B). To confirm further the distinct mobility of the two H2A.Z isoforms, recombinant H2A.Z-1 and H2A.Z-2 proteins were expressed in bacteria and purified. The recombinant H2A.Z-1 and H2A.Z-2 migrated during long SDS–PAGE with a mobility corresponding to that of the 'upper' and the 'lower' endogenous H2A.Z polypeptides, respectively (Figure 2C). In contrast, these recombinant isoforms were not separated by AUT–PAGE (Supplementary Figure S2). These results indicate that long-gel SDS–PAGE, but not AUT–PAGE, can distinguish the chicken H2A.Z-1 and H2A.Z-2 polypeptides.

The relative level of H2A.Z-1-deposition in H2A.Z-2-deficient cells and that of H2A.Z-2 in H2A.Z-1-deficient cells was slightly increased, although the difference was not statistically significant (Figure 2B). This might be because there is only a limited number of undeposited molecules of each H2A.Z isoform, or alternatively because the machineries for the deposition of each H2A.Z isoform are distinct.

H2A.Z isoforms are deposited into chromatin by the SRCAP complex to a similar extent

Two isoforms of H2A.Z are expressed in vertebrates, and the SRCAP and p400 complexes mediate H2A.Z deposition (8–10,29; Ohfuchi *et al.*, manuscript submitted for publication). These findings raise the possibility that each of these complexes acts specifically on one of the two H2A.Z isoforms. Such a scenario could explain a similar level of deposition of each H2A.Z isoform even in the absence of the other isoform (Figure 2B). The actin-related protein, Arp6, is a conserved and essential component of the SRCAP complex, but is not present in the p400 complex (9,10,30). Recently, we established a tet-inducible, Arp6-deficient DT40 cell line (Ohfuchi *et al.*, manuscript submitted). The activity of the SRCAP complex is expected to be impaired in Arp6-deficient cells. We next used this cell line to investigate whether the SRCAP complex exhibits specificity for one of the H2A.Z isoforms.

In the tet-inducible, Arp6-deficient cell line, Arp6 protein becomes undetectable at 96 h after the addition of tet (data not shown). The chromatin fraction was prepared from such cells grown in the presence or absence of tet, and the deposition of H2A.Z-1 and H2A.Z-2 was evaluated (Figure 3A). We observed ~70% less deposition of both the H2A.Z-1 and H2A.Z-2 isoforms in Arp6-deficient cells (Figure 3, Arp6 KO+tet 96 h and Arp6 KO+tet 120 h), consistent with reduced activity of the SRCAP complex in Arp6-deficient cells. Thus, we observed no differential deposition of H2A.Z-1 and H2A.Z-2 in the chromatin fraction of Arp6-deficient cells (Figure 3). The relative level of expression of the *H2A.Z-1* and *H2A.Z-2* isoforms was similar in WT and Arp6-deficient cells (Supplementary Figure S6). Therefore, we conclude that the SRCAP complex does not exhibit specificity for either isoform, and that it is responsible for ~70% of their deposition into chromatin.

Although Arp6 is constitutively expressed in all tissues, its expression is particularly abundant in early developmental stages up until the stage 29 embryo, whereas a lower level of expression is detected in the stage 32 embryo and thereafter (31). Analysis of histones prepared from chicken embryo nuclei revealed a reduced level of the sum of the two H2A.Z isoforms in stage 32 embryos compared to the level detected at earlier stages (Figure 4A and B). Since the expression of mRNAs encoding H2A.Z-1 and H2A.Z-2 was not significantly decreased in stage 32 embryos (Supplementary Figure S7), the deposition of H2A.Z isoforms thus also correlated with Arp6 expression in embryos. However, comparison of the relative occupancy of H2A.Z-1 and H2A.Z-2 revealed a reduced level of H2A.Z-1 occupancy at later embryonic stages (Figure 4A), and this tendency towards reduced occupancy was confirmed by a statistical comparison of the relative amounts of H2A.Z-1 and H2A.Z-2 (Figure 4C). Since the mechanism of the deposition of H2A.Z isoforms appears to be redundant, the reduced level of deposition of H2A.Z-1 in stage 32 embryos might reflect differential stability of the two isoforms within the histone octamer under certain states of the chromatin (see 'Discussion' section).

Characterization of the properties of H2A.Z-1 and H2A.Z-2 knockout cells

Although the two H2A.Z isoforms appear to be functionally redundant, the differences in their amino acid sequences suggest that there might be differences in their activities. To test this possibility, we compared cell growth and gene expression in the H2A.Z-1- and H2A.Z-2-deficient cells. Both cell lines are viable, which also supports a functional redundancy to their activity. However, comparison of cell growth revealed that H2A.Z-2-deficient cells proliferated 20–30% more slowly than WT or H2A.Z-1-deficient cells (Figure 5A). We next compared the cell-cycle distribution of the WT and knockout cells by FACS scan analysis. We observed no differences in the distribution of cells between the G1-, S- and G2/M-phases (Figure 5B). However, we observed an increase in the number of apoptotic H2A.Z-2-deficient cells (Figure 5C), which might explain the observed slower rate of growth of these cells. This suggests that H2A.Z-2, but not H2A.Z-1, might inhibit apoptosis.

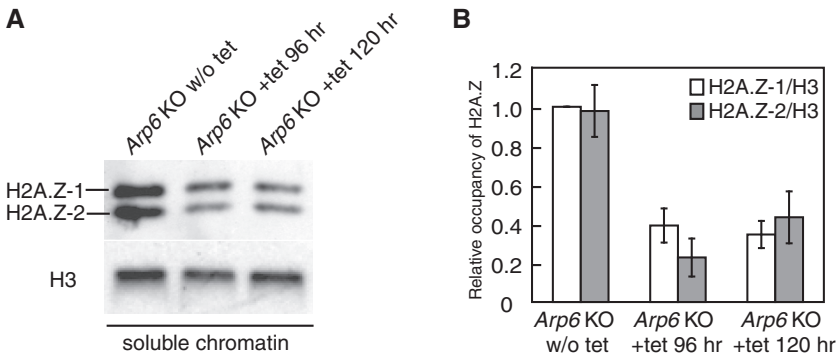

Figure 3. Impairment of the deposition of H2A.Z-1 and H2A.Z-2 in SRCAP complex-deficient cells. (**A**) The soluble chromatin fraction was prepared from tet-inducible Arp6-deficient cells before or after tet treatment (96 or 120 h). The deposition of H2A.Z isoforms was detected by western blot analysis following electrophoresis through a long-gel (upper panel). H3 histone was detected as a control in each fraction (Lower panel). The position of H2A.Z-1 and H2A.Z-2 are indicated at the left. (**B**) The signals corresponding to H2A.Z-1 and H2A.Z-2 were quantified and normalized to that of H3 histone. The relative deposition of the H2A.Z isoforms in each fraction is compared to that observed for H2A.Z-1 prior to induction of Arp6-deficiency in the graph. The error bars represent the mean ± standard deviation from at least three independent experiments.

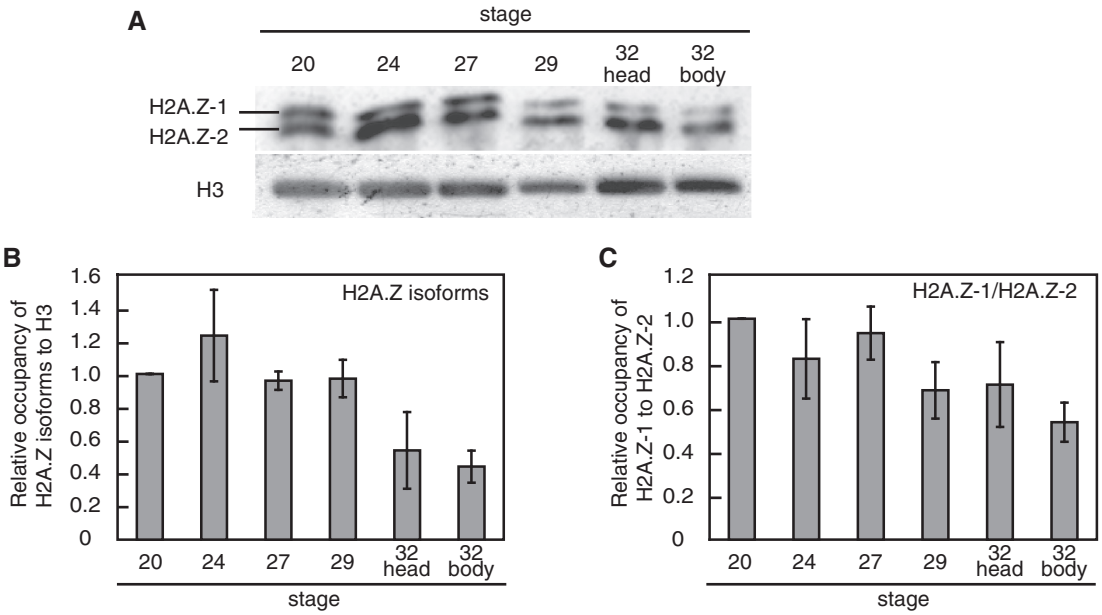

Figure 4. Occupancy of H2A.Z-1 and H2A.Z-2 at various developmental stages of the chicken embryo. (**A**) The histone fraction was prepared from stage 20 to 32 (3–7-days) chicken embryo. The histones were subjected to western blot analysis using anti-H2A.Z (upper panel) and anti-H3 (lower panel) antibodies. The stage of the embryo is indicated above the panels as the number of stage of embryogenesis. (**B**) Quantification of the occupancy of H2A.Z isoforms in chicken embryos. The sum of the deposition of H2A.Z-1 and H2A.Z-2 was calculated, and is indicated with the occupancy at stage 20 defined as 1.0. (**C**) The occupancy of H2A.Z-1 relative to that of H2A.Z-2 is shown, with the ratio at stage 20 defined as 1.0. The error bars represent the mean ± standard deviation from at least three independent experiments.

DT40 is a chicken B-cell lineage in which genetic recombination occurs frequently. Therefore, DT40 cells must attenuate certain DNA damage sensing pathways to escape from apoptosis. BCL6 is known to directly repress the DNA-damage sensor ATR and its downstream signaling pathway (32–35). We observed greatly decreased expression (<1/50) of the *BCL6* gene in H2A.Z-2-deficient cells (Figure 6A). This decrease in the expression of BCL6, a suppressor of apoptosis, might explain the increased apoptotic index of H2A.Z-2-deficient cells. *BCL6* gene transcription is reduced by the expression of the *IRF4* gene, which encodes a transcription repressor (36). Importantly, *IRF4* expression was not increased significantly in H2A.Z-1 deficient cells (<2-fold, Figure 6A). These observations suggest that the H2A.Z isoforms have differential effects upon *BCL6* expression, in a manner independent of IRF4 expression.

It has been shown that acetylation of lysine residues of H2A.Z is involved in its function, including its role in the regulation of transcription (5,37–40). Indeed, three of four substitutions of amino acids between chicken H2A.Z-1 and H2A.Z-2 are adjacent to lysine residues (Supplementary Figure S1 and see Discussion section). We compared the migration of H2A.Z isoforms by long-gel SDS–PAGE after induction of histone hyper-acetylation. H2A.Z-1- and H2A.Z-2-deficient cells were treated with tricostatin A (TSA), an inhibitor of HDAC, and chromatin was induced into a hyper-acetylated state. When the nuclear histone fraction prepared from the TSA-treated cells was analyzed, we observed the presence of more slowly-migrated polypeptides, which we assumed to be acetylated H2A.Z isoforms (arrows, Figure 6B). However, whereas the shift in mobility of the acetylated H2A.Z-2 isoform (arrow in H2A.Z-1-deficient, Figure 6B) was only slight, the shift in mobility of the acetylated H2A.Z-1 (arrow in H2A.Z-1-deficient, Figure 6B) was significant. This implies that the two H2A.Z isoforms were differentially acetylated under the conditions used and/or that their structures are differentially affected by their acetylation (see 'Discussion' section). Although this finding needs further investigation, the differential behavior of the two isoforms in the TSA-treated cells could possibly underlie their different effects upon gene expression.

DISCUSSION

H2A.Z-1 and *H2A.Z-2* genes are found in the genome of most vertebrates (24). However, the significance of the existence of two H2A.Z genes has yet to be determined. In most studies to date, the *H2A.Z-1* gene and its product have been analyzed. Here, we show that two distinct H2A.Z gene products are present in vertebrate cells. Since the two H2A.Z isoform genes and their products show high similarity, it is possible that some of the previously observed characteristics assigned to H2A.Z-1 may have been derived from the presence of H2A.Z-2. For example, siRNAs targeted to H2A.Z-1 would also target H2A.Z-2 owing to sequence similarity. In addition, the commercially available antibodies cannot distinguish the two isoforms. Here we established H2A.Z-1- and H2A.Z-2-KO cells in order to analyze the distinct characteristics of H2A.Z-1 and H2A.Z-2. We were able to separate the two H2A.Z isoforms using long-gel SDS–PAGE

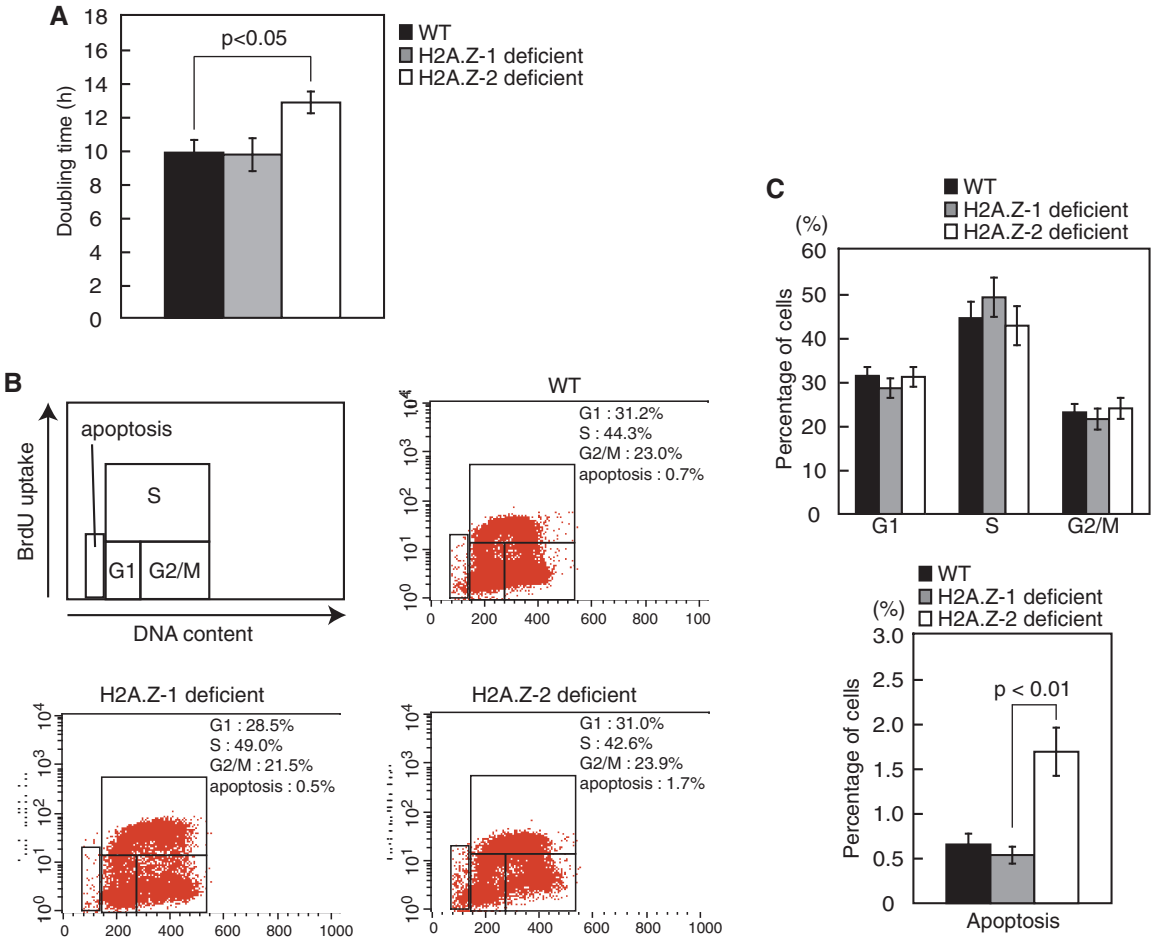

Figure 5. Comparison of DT40 cells deficient in each of H2A.Z isoforms. (**A**) Comparison of the growth of WT, H2A.Z-1- and H2A.Z-2-deficient cells. Trypan blue staining was used to discern dead and living cells and the latter were counted. Doubling times were estimated from the growth curves. (**B**) Cell cycle distribution of WT, H2A.Z-1- and H2A.Z-2-deficient cells. Cells were stained with the FITC-anti-BrdU conjugate (*y*-axis, log scale) to quantify BrdU incorporation (BrdU duration: 20 min) and with 7-AAD to quantify total DNA content (*x*-axis, linear scale). In each panel, the lower left box, the upper box and the lower right box represent regions containing G1, S and G2/M phase cells, respectively. The region on the far lower left of each graph shows apoptotic cells. The numbers given in the boxes indicate the mean percentages of each gated event. (**C**) The mean percentages of gated events containing G1, S and G2 cells (upper panel) and containing apoptotic cells (lower panel) were compared between WT, H2A.Z-1- and H2A.Z-2-deficient cells. The increase of the apoptotic index in H2A.Z-2-deficient cells is statistically significant ($P < 0.01$). The error bars represent the mean ± standard deviation from at least three experiments.

and were further able to identify these as H2A.Z-1 and H2A.Z-2 by using individual gene knockouts in DT40 cells.

The difference in the rate of migration of the isoforms by long-gel SDS–PAGE gel cannot be explained simply by the difference in molecular mass of H2A.Z-1 and H2A.Z-2 (13 582 and 13 502 Da, respectively). Since the recombinant H2A.Z-1 and H2A.Z-2 proteins migrated with mobilities identical to those of their endogenous counterparts, post-translational modifications cannot explain the differential mobility. Therefore, it seems likely that a structural difference based on the amino acid substitutions between the isoforms might underlie the differential mobility during SDS–PAGE.

Both H2A.Z isoforms were deposited by the SRCAP complex to a similar extent (Figure 3), suggesting that the H2A.Z isoforms are functionally redundant to some extent. Indeed, ectopic overexpression of H2A.Z-1 reduced the amount of H2A.Z-2 in chromatin (data not shown). On the other hand, the levels of the two H2A.Z isoforms appear to be independently controlled, even in the absence of the other isoform (Figure 2B). This finding suggests that there is only a small (or restricted) cellular fraction of undeposited molecules of each isoform. Quantitative shifts in the fraction of undeposited molecules by changes in their transcription under certain circumstances might be expected to enhance or neutralize the differential effects of the H2A.Z isoforms.

Analyses of H2A.Z-1- and H2A.Z-2-deficient cells suggested that the isoforms also exhibit specific properties. The differences in the amino acid sequences of the chicken H2A.Z isoforms are located adjacent to the K12, K14 and K16 residues (T/A13 and T/A15) and the K38 residue (S/T39), and at the C terminus (V/A128) (Supplementary Figure S1). At least the five lysine residues in the N-terminal tail, including K12, K14, and

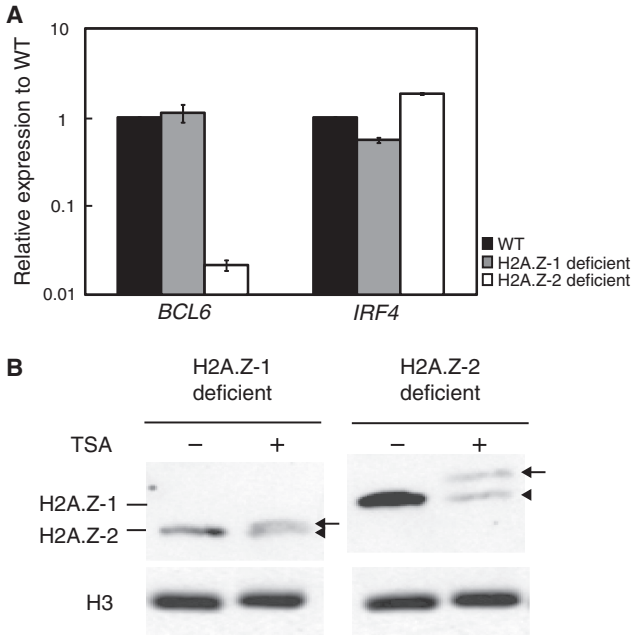

Figure 6. Different properties of the H2A.Z isoforms. (**A**) Decrease in the expression of the *BCL6* gene in H2A.Z-2-deficient cells. Expression of *BCL6* and *IRF4* genes in WT, H2A.Z-1- and H2A.Z-2-deficient cells was compared by real-time quantitative RT-PCR analysis. The signals corresponding to the *BCL6* and *IRF4* mRNAs were normalized to that corresponding to the *β-actin* mRNA. The relative expression of these genes in H2A.Z-deficient cells compared to WT cells is plotted in log scale. The error bars represent the mean ± standard deviation from three experiments. (**B**) Mobility of the H2A.Z isoforms by long-gel SDS–PAGE after induction of histone hyperacetylation. H2A.Z-1- and H2A.Z-2-deficient cells were cultured in the presence of 500 nM tricostatin A (TSA) for 12 h. The chromatin fractions from control (TSA−) and TSA-treated (TSA+) cells were subjected to detection of H2A.Z-1 (right panel) and H2A.Z-2 (left panel) by long-gel SDS–PAGE. The positions of the H2A.Z isoforms in control cells (arrowhead) and the shift in the mobility of the polypeptides following induction of histone hyperacetylation (arrow) are shown.

K16, of the H2A.Z isoforms are acetylated *in vivo* (26,27). The shift in mobility of the H2A.Z isoforms following treatment of the cells with TSA suggests that they are differentially acetylated and/or that their structures are differentially affected by their acetylation, such that the mobility shift of H2A.Z-1 is greater than that of H2A.Z-2 (Figure 6B). Since it has been shown that the N-terminal tails of the two isoforms are acetylated to a similar extent (26), it appears that the conformation of the two isoforms may be differentially affected by the acetylation. However, we cannot exclude the possibility that the acetylation of K38 adjacent to the S/T39 substitution may differ between the H2A.Z isoforms. Acetylated H2A.Z is associated with various gene functions including transcriptional activation, prevention of heterochromatin spreading, chromosome transmission and DNA repair (37–39). The H2A.Z isoforms might contribute differentially to gene function through their distinctive behavior following acetylation.

Genome-wide distribution analysis has revealed that H2A.Z is deposited together with histone variant H3.3 at active promoters, enhancers, and insulators. Nucleosome-free regions (NFRs) are occasionally observed within such regions of the genome (16). Nucleosome core particles containing H2A.Z and H3.3 have been shown to be less stable than those containing only H2A.Z or canonical H2A (41). Therefore, a H2A.Z/H3.3 double variant-containing nucleosome is likely to induce the presence of NFRs (16,23). H2A.Z and H3.3 located within promoters and enhancers are expected to be involved in transcriptional regulation through the formation of NFRs. It is likely that the combination of H3 and H2A.Z isoforms contributes to multiple modes of gene regulation.

Here we showed differential effects of individual knockouts of the H2A.Z isoforms on *BCL6* gene expression (Figure 6A). BCL6 is required for the suppression of apoptosis and the maturation of B cells. BCL6 can also act as a proto-oncogene (42). BCL6 expression is repressed by the binding of the IRF4 transcriptional repressor to its gene (36). However, reduced expression of the *BCL6* gene ($<1/50$) in H2A.Z-2-deficient cells was not accompanied by increased expression of the *IRF4* gene. Taken together with the stable occupancy of H2A.Z-2 in embryos (Figure 4), H2A.Z-2-containing nucleosomes may be relatively resistant to the formation of NFRs and may thus prevent efficient binding of the IRF4 repressor. Although we need to test this possibility further, the *BCL6* gene may represent an appropriate model to investigate the role of H2A.Z-2 in transcriptional regulation. Whereas *BCL6* gene expression was unaffected in H2A.Z-1-deficient cells, we have identified two genes whose expression is decreased in the absence of H2A.Z-1 (Supplementary Figure S8). These genes could be utilized to clarify the specific properties of the H2A.Z isoforms in transcriptional regulation. Differential association of the isoforms with methylated H3 histone (26) might contribute to their specific effects upon the expression of certain genes.

H2A.Z has been extensively studied in recent years, and its significance in the regulation of genome function is generally recognized. Whereas knowledge of the expression and activity of H2A.Z in germ cells and embryos is limited, it has been suggested that it may have important roles in development and cell differentiation (4). However, the role of H2A.Z in transcriptional regulation remains controversial (40). Further analyses of expression and activity of H2A.Z isoforms should provide new insight into the mechanisms of genome regulation by histone variants.

SUPPLEMENTARY DATA

Supplementary Data are available at NAR Online.

ACKNOWLEDGEMENTS

The authors thank Dr Hiroshi Kimura and Dr Masahiro Okada for discussion and technical assistances.

FUNDING

Funding for open access charge: Grants-in-Aids for Scientific Research of Priority Areas and for Scientific Research on Innovative Areas from the Ministry of Education, Culture, Sports, Science, and Technology, Japan.

Conflict of interest statement. None declared.

REFERENCES

1. Luger,K., Rechsteiner,T.J., Flaus,A.J., Waye,M.M. and Richmond,T.J. (1997) Characterization of nucleosome core particles containing histone proteins made in bacteria. *J. Mol. Biol.*, **272**, 301–311.
2. Kornberg,R.D. and Lorch,Y. (1999) Twenty-five years of the nucleosome, fundamental particle of the eukaryote chromosome. *Cell*, **98**, 285–294.
3. Altaf,M., Auger,A., Covic,M. and Côté,J. (2009) Connection between histone H2A variants and chromatin remodeling complexes. *Biochem. Cell Biol.*, **87**, 35–50.
4. Santenard,A. and Torres-Padilla,M.E. (2009) Epigenetic reprogramming in mammalian reproduction: contribution from histone variants. *Epigenetics*, **4**, 80–84.
5. Ren,Q. and Gorovsky,M.A. (2001) Histone H2A.Z acetylation modulates an essential charge patch. *Mol. Cell*, **7**, 1329–1335.
6. Van Daal,A. and Elgin,S.C. (1992) A histone variant, H2AvD, is essential in Drosophila melanogaster. *Mol. Biol. Cell*, **3**, 593–602.
7. Faast,R., Thonglairoam,V., Schulz,T.C., Beall,J., Wells,J.R., Taylor,H., Matthaei,K., Rathjen,P.D., Tremethick,D.J. and Lyons,I. (2001) Histone variant H2A.Z is required for early mammalian development. *Curr. Biol.*, **11**, 1183–1187.
8. Mizuguchi,G., Shen,X., Landry,J., Wu,W.H., Sen,S. and Wu,C. (2004) ATP-driven exchange of histone H2AZ variant catalyzed by SWR1 chromatin remodeling complex. *Science*, **303**, 343–348.
9. Wong,M.M., Cox,L.K. and Chrivia,J.C. (2007) The chromatin remodeling protein, SRCAP, is critical for deposition of the histone variant H2A.Z at promoters. *J. Biol. Chem.*, **282**, 26132–26139.
10. Ruhl,D.D., Jin,J., Cai,Y., Swanson,S., Florens,L., Washburn,M.P., Conaway,R.C., Conaway,J.W. and Chrivia,J.C. (2006) Purification of a human SRCAP complex that remodels chromatin by incorporating the histone variant H2A.Z into nucleosomes. *Biochemistry*, **45**, 5671–5677.
11. Albert,I., Mavrich,T.N., Tomsho,L.P., Qi,J., Zanton,S.J., Schuster,S.C. and Pugh,B.F. (2007) Translational and rotational settings of H2A.Z nucleosomes across the Saccharomyces cerevisiae genome. *Nature*, **446**, 572–576.
12. Guillemette,B., Bataille,A.R., Gévry,N., Adam,M., Blanchette,M., Robert,F. and Gaudreau,L. (2005) Variant histone H2A.Z is globally localized to the promoters of inactive yeast genes and regulates nucleosome positioning. *PLoS Biol.*, **3**, e384.
13. Li,B., Pattenden,S.G., Lee,D., Gutiérrez,J., Chen,J., Seidel,C., Gerton,J. and Workman,J.L. (2005) Preferential occupancy of histone variant H2AZ at inactive promoters influences local histone modifications and chromatin remodeling. *Proc. Natl Acad. Sci. USA*, **102**, 18385–18390.
14. Meneghini,M.D., Wu,M. and Madhani,H.D. (2003) Conserved histone variant H2A.Z protects euchromatin from the ectopic spread of silent heterochromatin. *Cell*, **112**, 725–736.
15. Raisner,R.M., Hartley,P.D., Meneghini,M.D., Bao,M.Z., Liu,C.L., Schreiber,S.L., Rando,O.J. and Madhani,H.D. (2005) Histone variant H2A.Z marks the 5′ ends of both active and inactive genes in euchromatin. *Cell*, **123**, 233–248.
16. Jin,C., Zang,C., Wei,G., Cui,K., Peng,W., Zhao,K. and Felsenfeld,G. (2009) H3.3/H2A.Z double variant-containing nucleosomes mark 'nucleosome-free regions' of active promoters and other regulatory regions. *Nat. Genet.*, **41**, 941–945.
17. Brickner,D.G., Cajigas,I., Fondufe-Mittendorf,Y., Ahmed,S., Lee,P.C., Widom,J. and Brickner,J.H. (2007) H2A.Z-mediated localization of genes at the nuclear periphery confers epigenetic memory of previous transcriptional state. *PLoS Biol.*, **5**, e81.
18. Zofall,M., Fischer,T., Zhang,K., Zhou,M., Cui,B., Veenstra,T.D. and Grewal,S.I. (2009) Histone H2A.Z cooperates with RNAi and heterochromatin factors to suppress antisense RNAs. *Nature*, **461**, 419–422.
19. Rangasamy,D., Berven,L., Ridgway,P. and Tremethick,D.J. (2003) Pericentric heterochromatin becomes enriched with H2A.Z during early mammalian development. *EMBO J.*, **22**, 1599–1607.
20. Rangasamy,D., Greaves,I. and Tremethick,D.J. (2004) RNA interference demonstrates a novel role for H2A.Z in chromosome segregation. *Nat. Struct. Mol. Biol.*, **11**, 650–655.
21. Hake,S.B. and Allis,C.D. (2006) Histone H3 variants and their potential role in indexing mammalian genomes: the "H3 barcode hypothesis". *Proc. Natl Acad. Sci. USA*, **103**, 6428–6435.
22. Henikoff,S., Henikoff,J.G., Sakai,A., Loeb,G.B. and Ahmad,K. (2009) Genome-wide profiling of salt fractions maps physical properties of chromatin. *Genome Res.*, **19**, 460–469.
23. Henikoff,S. (2009) Labile H3.3+H2A.Z nucleosomes mark 'nucleosome-free regions'. *Nat. Genet.*, **41**, 865–866.
24. Eirín-López,J.M., González-Romero,R., Dryhurst,D., Ishibashi,T. and Ausió,J. (2009) The evolutionary differentiation of two histone H2A.Z variants in chordates (H2A.Z-1 and H2A.Z-2) is mediated by a stepwise mutation process that affects three amino acid residues. *BMC Evol. Biol.*, **9**, 31.
25. Coon,J.J., Ueberheide,B., Syka,J.E., Dryhurst,D.D., Ausio,J., Shabanowitz,J. and Hunt,D.F. (2005) Protein identification using sequential ion/ion reactions and tandem mass spectrometry. *Proc. Natl Acad. Sci. USA*, **102**, 9463–9468.
26. Dryhurst,D., Ishibashi,T., Rose,K.L., Eirín-López,J.M., McDonald,D., Silva-Moreno,B., Veldhoen,N., Helbing,C.C., Hendzel,M.J., Shabanowitz,J. *et al.* (2009) Characterization of the histone H2A.Z-1 and H2A.Z-2 isoforms in vertebrates. *BMC Biol.*, **7**, 86.
27. Ishibashi,T., Dryhurst,D., Rose,K.L., Shabanowitz,J., Hunt,D.F. and Ausió,J. (2009) Acetylation of vertebrate H2A.Z and its effect on the structure of the nucleosome. *Biochemistry*, **48**, 5007–5017.
28. Fukagawa,T., Mikami,Y., Nishihashi,A., Regnier,V., Haraguchi,T., Hiraoka,Y., Sugata,N., Todokoro,K., Brown,W. and Ikemura,T. (2001) CENP-H, a constitutive centromere component, is required for centromere targeting of CENP-C in vertebrate cells. *EMBO J.*, **20**, 4603–4617.
29. Gévry,N., Chan,H.M., Laflamme,L., Livingston,D.M. and Gaudreau,L. (2007) p21 transcription is regulated by differential localization of histone H2A.Z. *Genes Dev.*, **21**, 1869–1881.
30. Wu,W.H., Alami,S., Luk,E., Wu,C.H., Sen,S., Mizuguchi,G., Wei,D. and Wu,C. (2005) Swc2 is a widely conserved H2AZ-binding module essential for ATP-dependent histone exchange. *Nat. Struct. Mol. Biol.*, **12**, 1064–1071.
31. Kato,M., Sasaki,M., Mizuno,S. and Harata,M. (2001) Novel actin-related proteins in vertebrates: similarities of structure and expression pattern to Arp6 localized on Drosophila heterochromatin. *Gene*, **268**, 133–140.
32. Ranuncolo,S.M., Polo,J.M. and Melnick,A. (2008) BCL6 represses CHEK1 and suppresses DNA damage pathways in normal and malignant B-cells. *Blood Cells Mol. Dis.*, **41**, 95–99.
33. Ranuncolo,S.M., Polo,J.M., Dierov,J., Singer,M., Kuo,T., Greally,J., Green,R., Carroll,M. and Melnick,A. (2007) Bcl-6 mediates the germinal center B cell phenotype and lymphomagenesis through transcriptional repression of the DNA-damage sensor ATR. *Nat. Immunol.*, **8**, 705–714.
34. Phan,R.T. and Dalla-Favera,R. (2004) The BCL6 proto-oncogene suppresses p53 expression in germinal-centre B cells. *Nature*, **432**, 635–639.
35. Phan,R.T., Saito,M., Basso,K., Niu,H. and Dalla-Favera,R. (2005) BCL6 interacts with the transcription factor Miz-1 to suppress the cyclin-dependent kinase inhibitor p21 and cell cycle arrest in germinal center B cells. *Nat. Immunol.*, **6**, 1054–1060.
36. Saito,M., Gao,J., Basso,K., Kitagawa,Y., Smith,P.M., Bhagat,G., Pernis,A., Pasqualucci,L. and Dalla-Favera,R. (2007) A signaling pathway mediating downregulation of BCL6 in germinal center B

cells is blocked by BCL6 gene alterations in B cell lymphoma. *Cancer Cell*, **12**, 280–292.
37. Millar,C.B., Xu,F., Zhang,K. and Grunstein,M. (2006) Acetylation of H2AZ Lys 14 is associated with genome-wide gene activity in yeast. *Genes Dev.*, **20**, 711–722.
38. Keogh,M.C., Mennella,T.A., Sawa,C., Berthelet,S., Krogan,N.J., Wolek,A., Podolny,V., Carpenter,L.R., Greenblatt,J.F., Baetz,K. *et al*. (2006) The Saccharomyces cerevisiae histone H2A variant Htz1 is acetylated by NuA4. *Genes Dev.*, **20**, 660–665.
39. Babiarz,J.E., Halley,J.E. and Rine,J. (2006) Telomeric heterochromatin boundaries require NuA4-dependent acetylation of histone variant H2A.Z in Saccharomyces cerevisiae. *Genes Dev.*, **20**, 700–710.
40. Thambirajah,A.A., Dryhurst,D., Ishibashi,T., Li,A., Maffey,A.H. and Ausió,J. (2006) H2A.Z stabilizes chromatin in a way that is dependent on core histone acetylation. *J. Biol. Chem.*, **281**, 20036–20044.
41. Jin,C. and Felsenfeld,G. (2007) Nucleosome stability mediated by histone variants H3.3 and H2A.Z. *Genes Dev.*, **21**, 1519–1529.
42. Dalla-Favera,R., Migliazza,A., Chang,C.C., Niu,H., Pasqualucci,L., Butler,M., Shen,Q. and Cattoretti,G. (1999) Molecular pathogenesis of B cell malignancy: the role of BCL-6. *Curr. Top Microbiol. Immunol.*, **246**, 257–263; discussion 263–265.